

Research Article

**APPLICATION OF 1-D SLOPE STABILITY MODEL IN LANDSLIDE
SUSCEPTIBILITY MAPPING OF SHIVKHOLA WATERSHED
DARJILING HIMALAYA**

***Sujit Mondal¹ and Ramkrishna Maiti²**

¹*Department of Geography Raja N. L. Khan Women's College
Paschim Medinipur West Bengal 721102*

²*Department of Geography and Environment Management
Vidyasagar University Paschim Medinipur West Bengal 721102*

**Author for Correspondence*

ABSTRACT

The present study deals with the assessment of geo-technical parameters i.e. surface inclination (α), soil depth (z), cohesion (c), angle of internal friction (ϕ), soil saturation index (m), Soil density (γ) and density of water (γ_w) and the application of 1D (one dimensional) Slope stability model to prepare the slope instability map under dry, semi-saturated and saturated condition of the landslide prone small hilly Shivkhola Watershed of Darjiling Himalaya. To determine the spatial distribution of slope instability in the watershed, safety factor value for 50 different locations were being estimated and with the help of GIS tools instability maps were being prepared. The probability or the chances of landslide phenomena in each class of slope instability maps were extracted by means of *frequency ratio* (FR) which shows that the probability/chances of landslide events could be expected as very high in the high to very high landslide susceptibility area and vice versa to all three conditions. The analysis of slope instability under three conditions also suggested that there was an aerial expansion of very high landslide susceptibility in comparison to dry and semi-saturated condition in saturated condition. This aerial expansion was the outcome of complete saturation and reduction of shearing strength of the slope materials above the failure plane surface. Finally, an accuracy assessment was made by ground truth verification of the existing landslide location where the classification accuracy for dry, semi-saturated and saturated conditions was 93.86%, 94.58% and 85.44% respectively.

Key Words: *1D Slope stability model, RS and GIS, Landslide Susceptibility, Safety Factor (FS), Frequency Ratio (FR), Accuracy Assessment*

INTRODUCTION

The factors conducive to slope instability, can be recognized at various levels of abstraction from the slope itself. The cohesion and pore-water pressure both directly control the magnitude of stress of the slope materials. These direct factors can be influenced by other factors recognized at successively more remote levels of abstraction. For example, pore-water pressure may be related to the rate of infiltration through the ground surface, which in turn, may be related to the density of vegetation cover which is again subject to change as a result of climatic conditions or land use activity. These chains of relationships may be critical in reducing the slope stability condition over time to a point where the triggering of movement may occur. Landslide susceptibility is thus a function of the degree of the inherent stability of the slope together with the intensity of causative factors capable of reducing the excess strength. Slope instability resulted from complex geological setting combined with various geomorphologic, hydrologic and geo-technical factors such as slope, relief, aspect, rainfall, drainage, upslope contributing area, cohesion, angle of internal friction, wet soil density, depth of the soil, shear stress, shear strength etc. So, the identification of the causative factors is the basis of many methods of landslide susceptibility assessment. In most of the cases, the landslide is the critical mechanism of erosional processes and in such condition landslide is inevitable and necessary part of the natural landscape process system. Although the occurrences of landslide hazards and its impact on human society cannot be prevented fully by analyzing the slope stability condition, but the better understanding of geo-

Research Article

technical attributes of the soil can contribute to greater knowledge and understanding about the spatial distribution of slope instability which are very much essential for land use planning.

The geotectonic factors of slope instability were studied in details by Brudsen, 1979; Windisch, 1991; Carson, 1975; Carson, 1977; and Borga *et al.*, 1998. Geomorphological relationship between landslide types and pattern and the morphological, lithological and structural settings were investigated by Guzzetti and Cardinali (1992), Barchi *et al.*, (1993) and Cardinali *et al.*, (1994) and then were summarized by Guzzetti *et al.*, (1996). Cardinali *et al.*, (2002b) presented a geomorphological approach to estimate landslide hazard and risk. The hydrologic factors like daily rainfall threshold in connection with slope angle and regolith thickness (Gabet *et al.* 2004), rainfall intensity and infiltration (Jakob and Weatherly, 2003) etc. were practiced in the analysis of slope instability. Several approaches to assess slope stability and landslide hazards were put forwarded by Montgomery and Dietrich, 1989; Carrara *et al.*, 1991; Hammond *et al.*, 1992; and Montgomery and Dietrich, 1994. Montgomery and Dietrich (1994) combined a contour based steady state hydrologic model with the infinite slope stability model (simplified for cohesion less soils) to define slope stability classes based upon slope and specific catchment area. The models in connection to the slope stability, shallow and deep seated landslides were introduced and verified by Varnes, (1958), Young (1963), Vanmarcke (1977) Hollingworth and Kovacs (1981), Burton and Bathrust (1998), Bradinoni and Church (2004), and Vleeschauwer & Smedt (2002), Smedt (2005) and Bhattarai *et al.*, (2001). The geotectonic factors of slope instability were studied in details by Brudsen, 1979; Windisch, 1991; Carson, 1975; Carson, 1977; and Borga *et al.* 1998. A comprehensive list of stability factors commonly employed in the factors mapping approach, given by Crozier (1986), Guzzetti *et al.*, (1999a, 1999a, 2003) and Tiwari and Marui (2001, 2002, 2003, 2004). An integrated approach for landslide susceptibility mapping using Remote Sensing and GIS produced by Sarkar and Kanungo (2004); Sharifikia (2007) Pande, Dabral, Chowdhury and Yadav (2008); and Nithya and Prasanna (2010). Lee and Choi 2003c; Chung and Fabri, 2003; Lee and Pradhan, 2006, 2007; Youssef *et al.*, 2009; Pradhan and Lee, 2010a, 2010b, 2010c; and Pradhan *et al.*, 2010a have studied and applied the probabilistic model in connection to RS and GIS for landslide susceptibility and risk evaluation.

A number of predictive as well as probabilistic models were used for identifying areas of landslide risk by Gokceoglu *et al.*, (2000); Pistocchi *et al.*, (2002); Lee, Choi and Min (2004); Barbieri & Cambuli (2009) and Bathurst *et al.*, (2010). The Landslide hazard risk and susceptibility in the mountainous region was studied using various model by Varnes (1984), Lee and Ryu (2004), Van Westen *et al.*, (2008), Vijith and Madhu (2008) and Kouli *et al.*, (2010). Atkinson and Massari (1998) applied a generalized linear model for analyzing landslide susceptibility.

The present study encompasses the assessment of geo-technical parameters of the collected soil samples from 50 landslide locations selected through stratified random sampling with representatives of different land uses and slope classes. The geo-technical attributes include surface inclination (β), soil depth (z), cohesion (c), angle of internal friction (ϕ), soil saturation index (m), Soil density (γ_s) and density of water (γ_w). The geometry of the slope, pore-water of the slope materials, angle of internal friction and cohesion are required to assess the stress parameters of the slope materials (Glade, 1998) and Safety Factor value. Before planning the land use pattern, the better understanding and investigation of geo-tectonic parameters and the preparation of a stability distribution map by applying GIS tools are very much popular and accepted approach in the present time. The prime motto of the present study is to study various geo-technical parameters and to prepare *landslide susceptibility maps* of the Shivkhola Watershed (Figure1) in dry, semi-saturated and saturated condition applying *1D slope Stability model* on GIS platform. The validity of the prepared landslide susceptibility maps in all conditions were evaluated by means of a *frequency ratio* (FR). Finally, an accuracy assessment was made by ground truth verification of the existing landslide location where the classification accuracy for dry, semi-saturated and saturated condition was 93.86%, 94.58% and 85.44% respectively.

Research Article

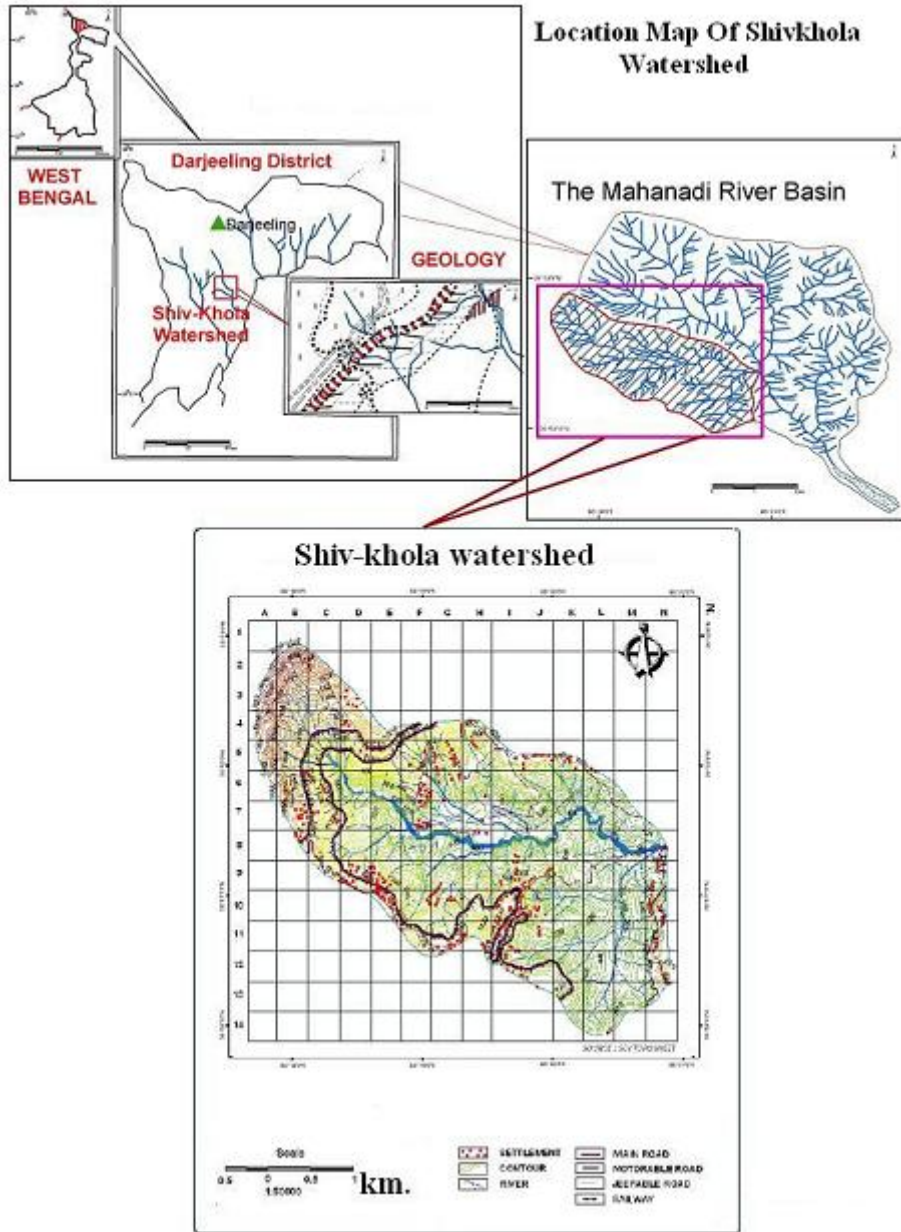


Figure1: Location Map of Shivkhola Watershed

MATERIALS AND METHODS

Slope Stability Model Concept

Two forces are responsible to determine the stability condition i.e. driving force (shear stress) and resisting force (shear strength). Shear stress is given as, $\tau = \gamma D \sin \alpha \cos \alpha$ and shear strength of Mohr and Coulomb defined as, $S = c + \tau \tan \phi$. Saturated slope material increases instability with increasing pore water pressure. The pore water pressure depends on unit weight of water (γ_w) and the height of water (D_w) above the failure plane surface. The height of the water shows the ground water condition in the soil. In this case the shear resistance of the soil is given by the following:

$$S = c + (\gamma - \gamma_w m) D \cos^2 \alpha \tan \phi \dots \dots \dots (\text{eq.1})$$

Research Article

Where, m is saturation index which shows the saturation condition of the soil. If the value of ‘m’ equals to ‘1’, the soil is completely saturated and the value of 0 indicates complete dry condition.

In many investigations of natural slope stability, infinite slope analysis had frequently been used because of its relative simplicity where the thickness of the soil is smaller than the length of the slope. For realistic modeling, 3D failure mechanism should be considered which includes different depth of sliding surface throughout the slope failure mass. A simplified approach was considered by Soeters and Westen (1996) reducing 3D depth to 2D equivalent depth based on equal factor of safety. However, it is not simple to analyze 2D rotational slide due to variation in depth of sliding surface. Hence, 2D depth of rotational slide (eq.2 & Figure2) was again converted to equivalent translational depth (1D) (eq.3 & Figure3) keeping the same factor of safety.

The stability analysis could be done in *1D Stability Model* without the impact of ground water using the following equation-3.

$$FS \text{ (Rotational)} = \frac{c + \gamma \cdot \tan \phi \sum_{i=1}^n z_i \cdot \cos^2 \beta}{\gamma \sum_{i=1}^n z_i \cdot \sin \beta \cdot \cos \beta} \dots \dots \dots (eq.2).$$

$$FS \text{ (Translational)} = \frac{c + \gamma \cdot z \cdot \cos^2 \beta \cdot \tan \phi}{\gamma \cdot z \cdot \sin \beta \cdot \cos \beta} \dots \dots \dots (eq.3).$$

[Where, γ = unit weight of the soil; z = depth of the failure surface below the terrain surface; β = the terrain surface inclination; ϕ = angle of internal friction; c = cohesion.].

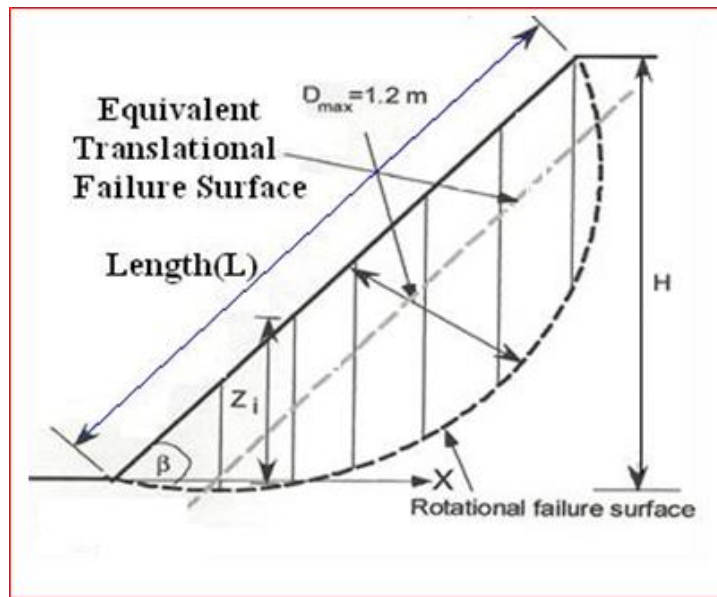


Figure: 2 Two Dimensional (2-D) Depth of Rotational Slide

The safety factor (FS) under the influence of ground water (semi-saturated and saturated condition) of cohesive soil has been considered in the present work applying the revised *1D slope stability model* (Figure3) with the help of following relationship (eq.7.4).

$$FS = \frac{c + (\gamma - m \cdot \gamma_w) \cdot \cos^2 \beta \cdot \tan \phi}{\gamma \cdot z \cdot \sin \beta \cdot \cos \beta} \dots \dots \dots (eq. 4)$$

[Where, γ =unit weight of soil; m =soil saturation index; Z_w = height of water table above failure surface; Z =depth of failure surface below the terrain surface; γ_w =unit weight of water; β =the terrain surface inclination; ϕ =angle of internal friction and c = cohesion.].

Research Article

slope stability. All the tests were carried out under drained condition. The major stress (σ_1), minor stress (σ_3) and cohesion (c) were estimated through tri-axial soil testing mechanism (Figure4) from Geo-technical Laboratory of GSI, Kolkata (22/com/soil/GTL/ER/O6-07) by Geologists Sufiyan, Sengupta, and Pramanik (2007). A Mohr Stress Circle was developed to obtain angle of internal friction and angle of rupture through σ_3 and σ_1 with the centre on the horizontal axis; the centre of the circle was obviously $(\sigma_1 + \sigma_3)/2$ and the radius was $(\sigma_1 - \sigma_3)/2$ [Figure5]. The values of confining pressure, σ_3 , and compressive stress, σ_1 were plotted on horizontal axis where stress difference is $\sigma_1 - \sigma_3$. On a plane parallel to the greatest principal stress axis ($2\alpha=0$) the normal stress across the plane was σ_3 and the shearing stress was 0. If the plane makes an angle of 45° with the greatest principal stress axis ($2\alpha=90$), the shearing stress is at a maximum and the normal stress is $(\sigma_1 + \sigma_3)/2$. If the plane makes an angle of 90° with the greatest principal stress axis ($2\sigma=180^\circ$), the shearing stress is 0 and the normal stress is σ_1 .

In this way a series of experiments were being accomplished with different values of confining pressure (σ_3). The Mohr Circle shows that as the confining pressure is increased, the stress as well as the stress difference must be increased to produce rupture. A line which is the tangent of the 'Mohr Circle' is called as the 'Mohr Envelope'. The angle that this line makes with the horizontal axis of the diagram is the angle of internal friction, ϕ (Figure5). Along any potential plane of rupture within a rock:

$$\mu = \tau/n = \tan\phi \dots\dots\dots(\text{eq.9})$$

Where μ is the coefficient of internal friction,
 τ = shearing stress along plane,
 n = normal stress along the lane,
 ϕ = the angle of internal friction.

The τ is at a maximum when $\alpha=45^\circ$; whereas n is at a minimum when $\alpha=0$ and at a maximum when $\alpha=90^\circ$. Shear fracture develop when n and τ combine to make the shear stress most effective. Since actual shear fracture make an angle of less than 45° with the greatest principal stress axis.

The intercept on the vertical axis, τ_o , is the cohesive strength of the rock. The curve for the Mohr envelope is –

$$\tau = \tau_o + \sigma_n \tan\phi \dots\dots\dots(\text{eq.10}).$$

Where, the angle that fractures should theoretically make with the greatest principal axis is

$$\alpha = \pm 45 \pm \phi/2 \dots\dots\dots(\text{eq.11}).$$

So, if the angle of internal friction is 30° , the fractures would make the angle of 30° with the greatest principal stress axis. On the other hand the shear fracture should theoretically form at 30° (Billings, 1987). Cohesion (C) is the attraction of particles to each other which is not directly governed by a FRICTION law but does provide a measure of strength of a material. Thus sands do not exhibit cohesion, while soil which contains clay show cohesion. It can be measured, as in soil mechanics, by the MOHR-COULOMB EQUATION (eq.12).

$$C(\text{cohesion}) = \frac{\sigma_1 - \sigma_3 \tan^2(45 + \frac{\phi}{2})}{2 + \tan(45 + \frac{\phi}{2})} \dots\dots\dots(\text{eq.12}).$$

Surface Inclination/Slope (B)

Slope gradients are sometimes considered as an index of slope instability, and because of the availability of a digital elevation model (DEM; Figure), slope can be numerically evaluated and depicted spatially (O' Neill and Mark, 1987; Gao, 1993). Firstly, the contour map at 20 meter interval was prepared and digitized from the topographical map 73B/8 (1987) at the scale of 1:50000 and subsequently used for generating Digital Elevation Model on ARC GIS platform. Then slope gradient map (Figure6) was

Research Article

extracted from DEM at 25m grid cell size and it was the classified after Anbalagan (1992) and Dhakal *et al.*, (2000).

Soil saturation Index/wetness index (*m*):

Simple models have been developed for estimating the soil saturation of the mountainous region as the wetness index is defined in TOPMODEL by Beven and Kirkby (1979).

$$m = \ln \frac{a}{\tan \theta} \quad \text{..... (eq. 13)}$$

Where *a*, is the contributing area per unit contour length and θ is the slope of the pixel.

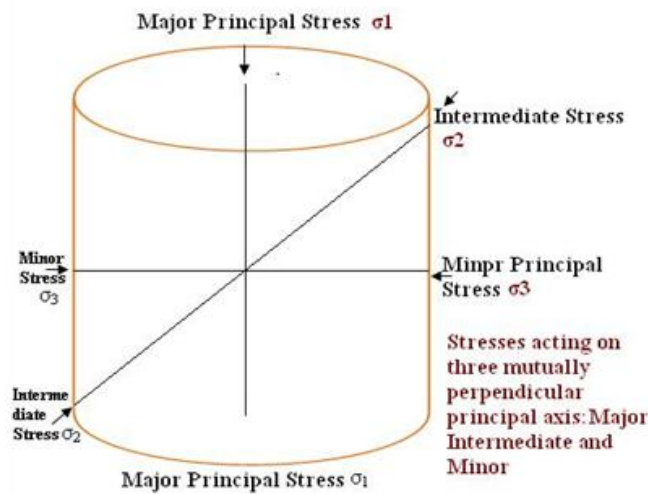


Figure 4: Soil Testing Mechanism Through Solid Cylinder Compression

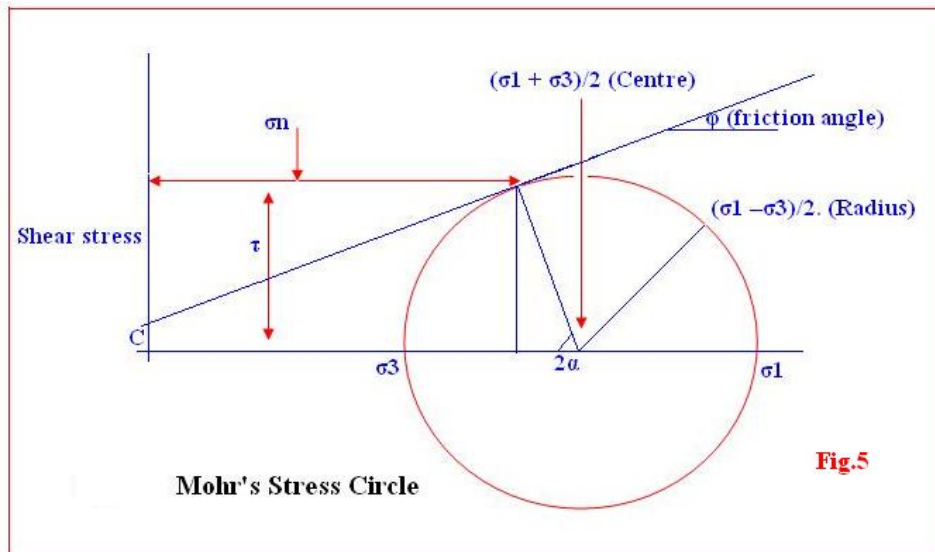


Figure: 5 Development of Mohr Stress Circle and Geo-technical Parameters.

Research Article

More acceptable soil saturation model was applied by Montgomery and Dietrich (1994), Borga *et al.*, (1998) and Pack and Tarboton (1998). The model envisages that the soil saturation index can be determined with the help of topography, soil type, and rainfall intensity of the area to be studied. But in practical sense, the soil is not completely dry or fully saturated in the area, therefore it can be imagined that the soil is half saturated. The soil saturation index is either fixed for stationary scenarios i.e. dry, semi-saturated and full saturated soils, given by $m = 0, 0.5$ and 1.00 or can be calculated on the basis of available rainfall data (De Smedt, 2005). On the basis of this assumption, wetness index equation can easily be derived and it is possible to see the effect of few days' consecutive rainfall in one day, if the soil is half saturated. In the present study wetness index (m) value of $0.00, 0.50$ and 1.00 under dry, half-saturated and full-saturated conditions were taken into account to make susceptibility maps.

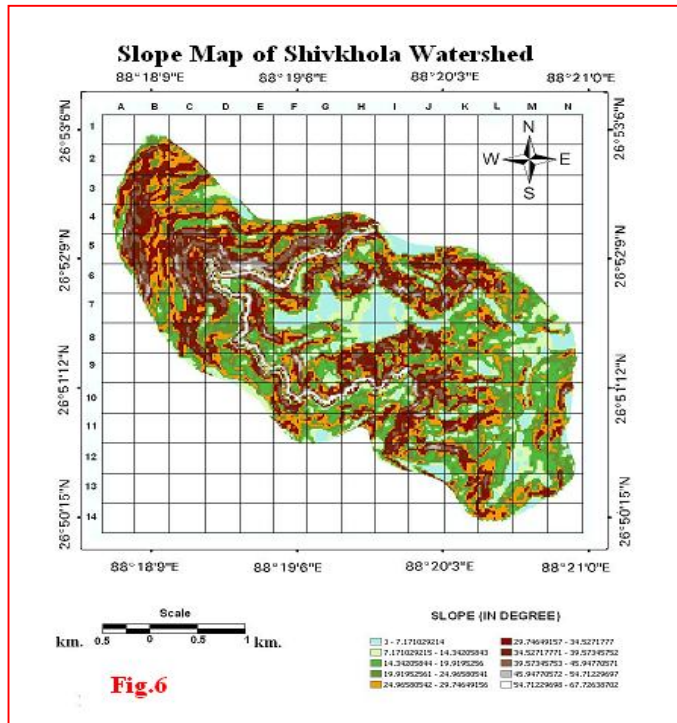


Figure: 6 Distribution of slope angle in the Shivkhola Watershed

Depth of failure surface/depth (z) of soil below the terrain surface:

Repeated and continued field studies for long duration were made for the proper cognition of the processes and their interaction. The depth of the failure surface was measured by holding a measuring tape at both the margins of scar and the other tape was allowed to hang, the reading was then taken from the base of the hanging tape. The margin of the scars was surveyed by *prismatic compass*. The intensive survey of the sliding scar for 40 different landslide locations was carried on by *Abney's level* at 0.5m interval along radial lines originating from lower most part of the scar. The altitude of the points at 0.5m interval along the radial lines is then estimated using Sine rule in reference to the central base point of known altitude determined by GPS (Basu and Maiti, 2001 and Maiti, 2007). The total thickness of soil and that of saturated soil for 50 sites during monsoon were measured from slope cutting. After estimating the approximate depth of all known points, a soil depth map (z/D) was made using Arc GIS tool (Figure7).

Soil Density (F_s) And Density Of Water (F_w)

Specific unit weight of water and unit weight of the soil were estimated by examining the soil samples collected from 50 landslide locations during field investigation from the GSI (Geological Survey of India,

Research Article

East Kolkata) laboratory. The density of soil and water varies from place to place due to in situ geo-hydrologic condition. The saturated soil density of rock was also consulted and adopted from the field experiences done by Deoja (Mountain Risk Engineering Handbook, 1991) and Specific Yield from Basic Ground-water Hydrology (Ralph C. Heath, 1991).

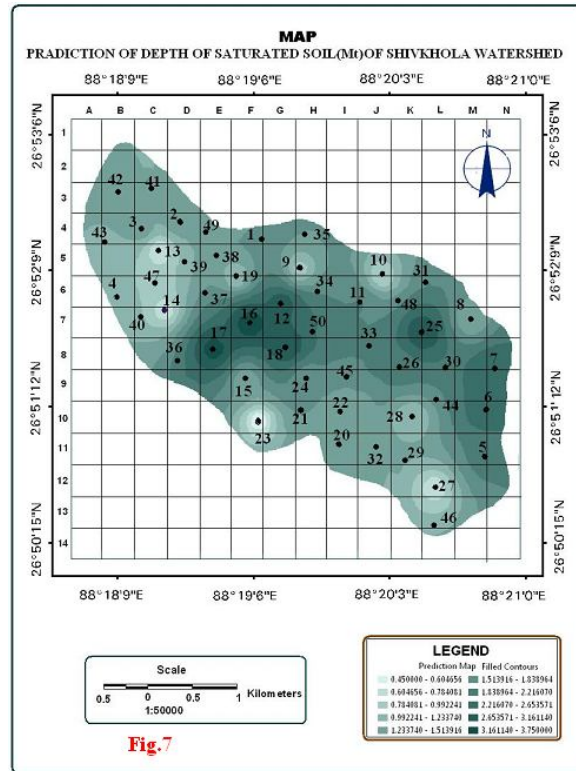


Figure: 7 Soil depth map of Shivkhola Watershed

Preparation Of Landslide Inventory Map For Accuracy Assessment

To determine the frequency ratio (FR) and to assess the overall classification accuracy, the major landslide location of the Shivkhola Watershed was detected by intensive field investigation with GPS, clinometers, and Abney’s level. Besides, LISS- III Satellite Image (2010), SRTM data (2008) and Google earth image (2010) had been incorporated with the surveyed landslide locations by thorough rectification and it was then modified and mapped accordingly (Figure8).

Application of 1 Dimension slope stability model and landslide susceptibility:

With the help of derived geo-technical parameters i.e. cohesion, friction angle, slope angle, unit weight of the soil, unit weight of water, soil depth, and saturation index value from 50 landslide location points of the Shivkhola watershed the *safety factor values* (FS) for dry, semi-saturated and saturated condition were being estimated by applying the 1D *slope Stability model* (Figure9 & eq.4). The safety factor values were transformed into raster value domain on ARC GIS Platform. Finally, the landslide susceptibility maps/safety factor distribution maps were prepared by ‘slicing’ operation and then stability classes for each condition (dry, semi and saturated condition) had been performed by studying the cumulative frequency and their abrupt change points of the safety factor values (the instability threshold boundaries). A 3×3 ‘majority filter’ technique was also applied to all the prepared safety factor distribution maps as a post-classification filter to reduce the high frequency variation. Higher the value of ‘FS’, greater is the propensity of slope stability and vice versa. To assess the chances/probability of landslide phenomena in each class to all the prepared maps under various conditions frequency ratio (FR) was extracted by means of a ratio between landslide frequency/landslide events (%) and landslide susceptibility area (%). FR

Research Article

value is approaching to 1 indicates equal chances of landslide events, 0 indicates lesser chances and more than 1 shows greater probability of landslide events.

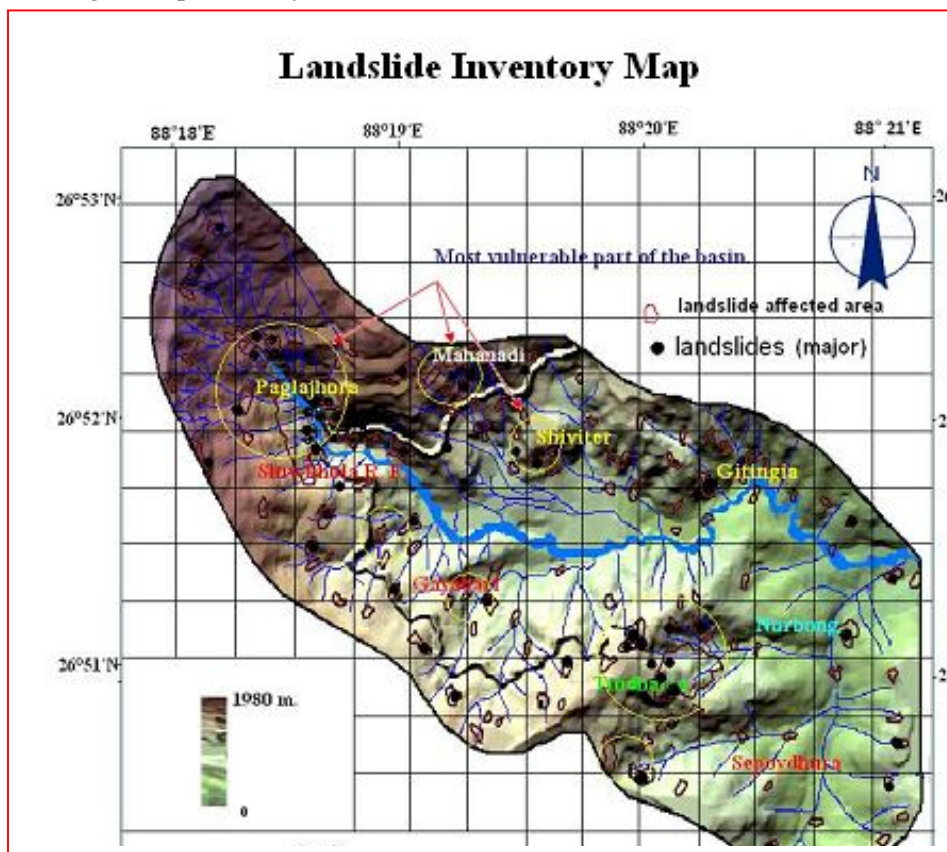


Figure: 8 Distribution of landslides in the Shivkhola Watershed

RESULTS AND DISCUSSION

Comparative Stability Analysis between Dry, Semi-Saturated And Saturated Soil Condition Based On 1d Slope Stability Model

The Shivkhola watershed exhibits a wide range of elevation (300 m to 2400 m). Slope ranges between very gentle of 7° and very high of 65° . The central middle section and lower section of the watershed is attributed with very gentle slope gradient of less than 20° whereas marginal part and extreme north, south and west are characterized by very steep slope of more than 50° . Angle of internal friction varies between 18° and 33° . Slope materials having coarse grains over the steep slope shows lower friction angle than the materials with finer particles deposited along the foothills zone. At lower and upper Paglajhora, Tindharia upslope, Shiviter and Nurbong the friction angle and cohesion of the soil is very low. Cohesion of the soil is high in the mid and lower part where more than 50% particles are composed with finer particles. The derived geo-technical parameters are in detail in the table.1.

The depth of soil varies from 0.45m to 3.75m in the Shivkhola watershed. The central mid-section and lower part of the watershed are registered with maximum soil depth whereas marginal part (north, south and western part) is attributed with minimum soil depth. Due to steep slope and active soil erosion process, the marginal area is associated with close slip surface below the slope surface due to which soil layers get saturated very easily and causes shallow debris slide. Tindharia, Gayabari upper, Sepoydhura upslope, upper Paglajhora, Mahanadi, Shiviter, Gitingia are existing in the marginal minimum soil depth

Research Article

area of the shivkhola watershed. on the other hand, shivkhola r.f., and both sides of the main river is characterized by maximum soil depth with low intensity of landslide phenomena.

Table 1: Result of field measurement and laboratory test of soil samples observed and collected from different location of the watershed

Samp le no.	(Z in m.)	(□) Φ	(c) kg/cm ³	(γ in KN/m ³)	(γ _w - KN/m ³)	FS (Dry)	FS (semi)	FS (Saturated)	
1.	1.55	42°	28°	0.42	1.86	0.92	0.883	0.737	0.5916
2.	1.45	54°	23°	0.21	2.13	1.01	0.452	0.378	0.3052
3.	1.40	37°	27°30'	0.11	1.89	0.89	0.7773	0.6146	0.4519
4.	1.25	38°	31°	0.65	1.97	0.82	1.3687	1.2019	1.0351
5.	2.00	39°	26°	0.45	2.01	0.90	0.8312	0.6963	0.5615
6.	1.35	39°	19°	0.02	2.01	1.12	0.4402	0.3218	0.2033
7.	2.75	49°	19°30'	0.03	2.25	1.09	0.3176	0.2430	0.1685
8.	1.15	35°	25°15'	0.60	2.05	0.85	1.215	1.0756	0.9360
9.	0.85	66°	24°	0.04	1.95	0.76	0.2631	0.2245	0.1859
10.	0.75	64°	29°	0.71	2.04	0.79	1.448	1.3958	1.3435
11.	1.85	67°	24°	0.02	2.36	1.08	0.2017	0.1584	0.1152
12.	2.95	22°	28°	0.65	2.21	0.99	1.6033	1.3085	1.0137
13.	0.55	65°	21°15'	0.01	2.00	0.84	0.2050	0.1670	0.1289
14.	0.65	46°	22°	0.32	2.05	0.82	0.8708	0.7927	0.7147
15.	1.20	51°	23°	0.79	1.88	0.77	1.0597	0.9893	0.9189
16.	3.75	59°	28°	0.67	2.06	0.78	0.5159	0.4554	0.3949
17.	3.50	57°	29°	0.66	2.10	0.76	0.5565	0.4675	0.2569
18.	3.25	15°	22°	0.33	2.22	0.81	1.6907	1.4157	1.1406
19.	0.95	63°	25°	0.25	1.98	0.77	0.5661	0.5199	0.4737
20.	0.75	64°	22°	0.04	2.35	1.01	0.2546	0.2123	0.1699
21.	1.25	48°	21°	0.05	2.23	0.98	0.3817	0.3058	0.2298
22.	1.20	52°	20°	0.07	2.22	0.88	0.3385	0.2822	0.2352
23.	0.45	46°	26°	0.91	1.99	0.85	2.5050	2.4044	2.3038
24.	1.55	20°	29°	0.52	2.03	0.73	2.0372	1.7634	1.4895
25.	3.15	24°	25°	0.06	2.11	0.75	1.0716	0.88551	0.69937
26.	2.10	13°	24°	0.58	2.13	0.74	2.52008	2.18508	1.85008
27.	0.65	36°	27°	0.86	1.96	0.69	2.12086	1.99742	1.87398
28.	0.90	26°	25°	0.10	1.90	0.68	1.104495	0.784422	0.7623225
29.	1.20	37°	25°	0.25	2.30	0.91	.7041	.6021	.5001
30.	2.20	28°	31°	0.81	2.22	0.87	.9137	.8131	.7124
31.	1.70	38°	24°	0.41	1.99	0.54	.8197	.7423	.6650
32.	1.30	36°	29°	0.75	1.97	0.53	1.3788	1.2178	1.1735
33.	2.65	27°	23°	0.06	2.11	0.77	3.546	2.9152	2.2843
34.	1.75	35°	32°	0.48	2.05	0.81	1.1772	1.000	.8246
35.	1.15	39°	27°	0.51	2.40	1.05	.8783	.7582	.6382
36.	2.18	44°	21°	0.09	2.44	1.11	0.3323	0.2627	0.2874
37.	1.72	64°	22°	0.25	2.15	0.98	0.3686	0.3237	0.2788
38.	1.65	49°	33°	0.24	1.89	0.66	0.7199	0.6214	0.5228
39.	1.40	61°	24°	0.08	1.97	0.53	0.3152	0.2820	0.2488
40.	1.35	25°	19°	0.06	2.02	0.72	0.7958	0.6642	0.5326
41.	1.49	30°	21°	0.09	2.55	1.09	0.7196	0.5774	0.4353
42.	1.40	42°	31°	0.17	2.48	1.09	0.7658	0.6191	0.4725
43.	0.85	51°	20°	0.35	1.85	0.61	0.7499	0.7013	0.6527
44.	1.45	23°	30°	0.40	1.93	0.65	1.7576	1.5285	1.2995
45.	1.50	55°	20°	0.22	2.04	0.96	0.4078	0.3479	0.2879
46.	0.95	66°	27°	0.15	2.58	1.29	0.3915	0.3348	0.2781
47.	0.65	49°	25°	0.08	2.47	1.22	0.5060	0.4059	0.3057
48.	1.15	38°	18°	0.29	2.00	0.72	0.6757	0.6009	0.5260
49.	1.23	47°	27°	0.32	1.79	0.50	0.7665	0.7002	0.6338
50.	3.05	18°	26°	0.78	1.99	0.60	1.9384	1.7121	1.4858

Research Article

[Z=soil depth; α =slope angle; ϕ = angle of internal friction; c=cohesion; γ =specific yield of soil; γ_w = unit weight of water; and m^* =wetness index with 20 year return period of rainfall intensity;]

It can be inferred that shallow seated slope instability is intimately related with minimum soil depth with steep slope.

In dry condition, around 15 sq.km of the watershed is attributed by moderate to very low landslide susceptibility and only 5 sq.km. is characterized with high to very high landslide susceptibility with high frequency ratio. Under semi-saturated condition 0.88 sq.km area is attributed with high landslide susceptibility. The area of high and very high landslide susceptibility has been increased in saturated soil condition and around 2.5 sq.km area is registering high landslide susceptibility with high frequency ratio. For dry and semi-saturated condition, the area under high and very high landslide susceptibility is 5.36 sq.km. and 8.5 sq.km. Respectively and the area under low to very low landslide susceptibility is around 9 sq.km. and 5 sq.km. under saturated soil condition small area (3.5 %) is experienced with low landslide susceptibility having frequency ratio of 0.00. around 14 sq. km. out of total area (21 sq.km.) of the watershed is being characterized by moderate to very high landslide susceptibility. under saturated condition, around 6 sq.km areas show the moderate landslide susceptibility with frequency ratio value of 0.39. upper and lower paglajhora, tindharia, shiviter and nurbong are the places where landslide susceptibility ranges from high to very high.

Table 2: Frequency Ratio analysis for dry, semi-saturated and saturated soil condition

<i>Frequency ratio analysis under Dry Condition</i>						
Safety Factor	Landslide susceptibility	Area sq.km.	in % of area	landslide frequency	Frequency Ratio	
0.158-0.40	Very high	0.320933	1.58	8 (33.33%)	21.09	
0.40-0.70	High	5.045979	24.88	9 (37.5%)	1.50	
0.70-1.00	Moderate	6.136645	30.25	5 (20.83%)	0.67	
1.00-1.50	Low	6.602401	30.51	2 (8.33%)	0.27	
1.50-2.83	Very low	2.188175	10.79	0 (0.00%)	0.00	
<i>Frequency ratio analysis under Semi-saturated condition</i>						
0.158-0.40	Very high	0.88796	4.38	9 (37.5%)	8.56	
0.40-0.70	High	7.691486	37.88	10 (41.67%)	1.10	
0.70-1.00	Moderate	6.393539	31.47	4 (16.67%)	0.53	
1.00-1.50	Low	4.15209	20.44	1 (4.16%)	0.20	
1.50-2.83	Very low	1.169058	5.76	0 (0.00%)	0.00	
<i>Frequency ratio analysis under saturated condition</i>						
0.158-0.40	Very high	2.430299	11.97	12 (50%)	4.17	
0.40-0.70	High	7.985823	39.36	8 (33.33%)	0.85	
0.70-1.00	Moderate	6.406416	31.58	3 (12.5%)	0.39	
1.00-1.50	Low	2.763299	13.60	1 (4.17%)	0.31	
1.50-2.83	Very low	0.708297	3.50	0 (0.00%)	0.00	

Lower middle section and few places of extreme south are characterized by moderate to very low landslide susceptibility under all soil saturated condition (table 2).

Susceptibility Under Dry Condition

The distribution of various magnitude of slope stability in figure 9. Under dry condition reveals that only 1.58% area of the watershed is experienced with very high landslide susceptibility where the chance of landslide phenomena is also very high. The said area is attributed with frequency ratio value of 21.09. 24.88% area shows high landslide susceptibility in the watershed. Maximum area (30.25%) of the

Research Article

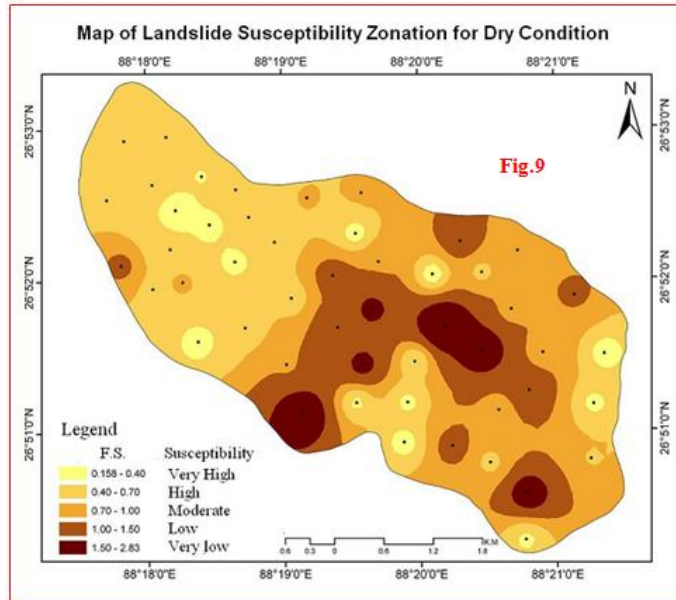


Figure9: Map of Landslide Susceptibility for Dry Condition

shivkhola watershed is dominated by moderate landslide susceptibility where the frequency of landslide is 20.835. more than 40% area of the shivkhola watershed falls under the low to very low landslide susceptibility with frequency ratio value of 0.27 and 0.00 respectively.

Susceptibility under Semi-Saturated Condition

Under semi-saturated condition the value of safety factor varies from 0.158 to 2.58 and 4.38 % area is under very high landslide susceptibility that is around 2.50 % greater than dry condition (Figure10).

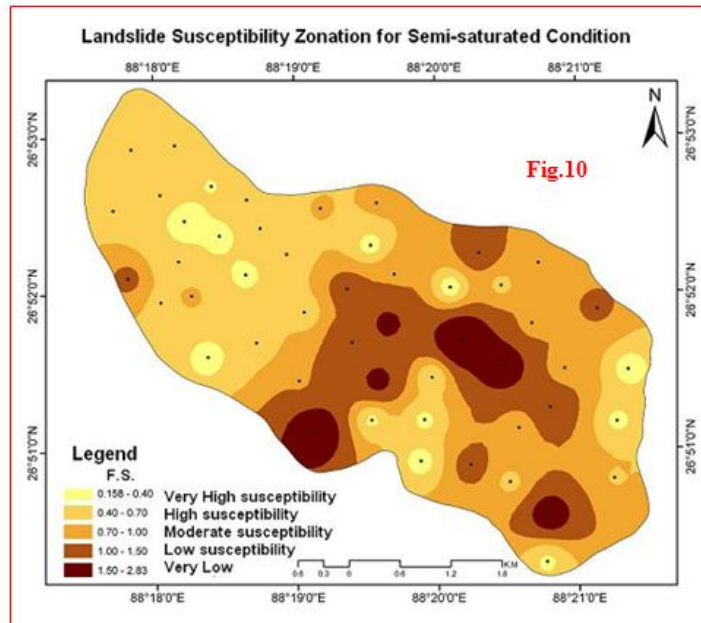


Figure10: Landslide Susceptibility Zonation for Semi-saturated Condition

Large part 37.88% area of the basin is dominated by high landslide susceptibility and 31.47 % area is registered with moderate landslide susceptibility and equal chances of landslide occurrence phenomena.

Research Article

More than 25 % of the watershed is exposed with low to very low landslide susceptibility condition. Frequency ratio value under semi-saturated condition revealed that the probability of landslide occurrence was very high in the area of very high landslide susceptibility which was followed by high, moderate and low. Under dry condition moderate, low and very low landslide susceptibility area had shown more or less absence of expected landslide phenomena as the derived frequency ratio values were approaching towards the value of '0'.

Susceptibility under Saturated Condition

Under the complete saturated soil condition pore water pressure becomes very high and reduces the cohesive strength of the soil and mountain slope become most unstable. The values of safety factor under saturated condition ranges between 0.13 and 2.30. The area of very high landslide susceptibility had been increased in comparison to dry and semi-saturated condition. More than 50% area of the Shivkhola watershed is attributed by high to very high landslide susceptibility. 31.585 % areas are under moderate landslide susceptibility where the probability of landslide activities is low. Under the saturated condition 11.97% area with very high landslide susceptibility shows the greater chances of landslide phenomena (Figure11).

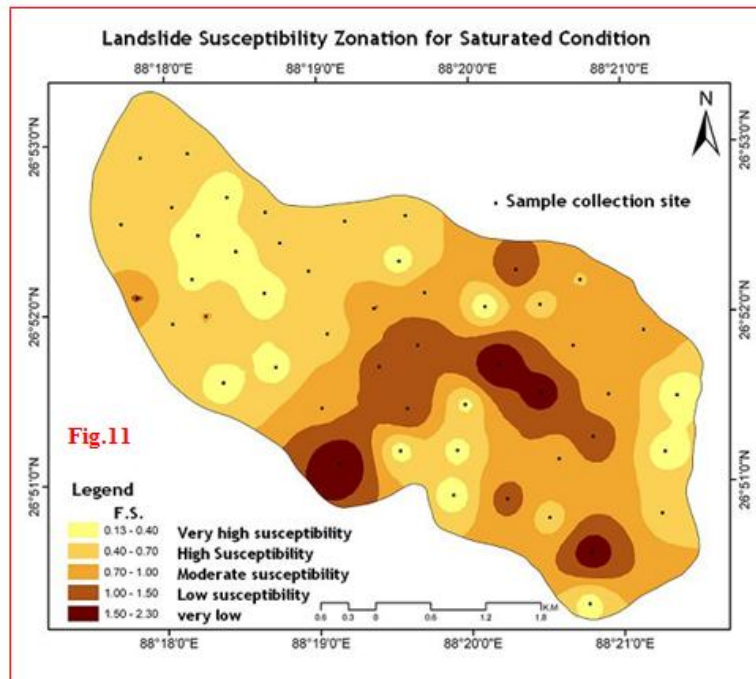


Figure11: Landslide Susceptibility Zonation for Saturated Condition

Extension of Very high landslide susceptibility under saturated condition is due to saturation of slope materials and heavy pore water pressure.

Accuracy Result

The comparison between assumed true data and randomly selected data from the classified image shows that the overall classification accuracy for dry, semi-saturated and saturated conditions are 93.86%, 94.58% and 84.44% respectively. The accuracy results in different landslide susceptibility classes under dry, semi-saturated and saturated conditions are stated in Table.3.

Research Article

Table.3: Accuracy Analysis.

Accuracy Study under Dry Condition					
Class name	Classified total	Number correct	Producers Correct	Users Accuracy	Accuracy Total.
Very low	0	6	0	0.00	0.00
Low	4	3	0	75	0.00
Moderate	10	9	9	90	100.00
High	17	15	14	88.23	93.33
Very High	18	17	15	94.44	88.24
Total =	50	50	38		
Overall classification Accuracy = 93.86%					
Overall Kappa Statistics = 0.8919					
Accuracy Study under Semi-saturated Condition					
Very low	0	6	0	0.00	0.00
Low	0	7	0	0.00	0.00
Moderate	13	10	9	76.92	90.00
High	20	16	16	80.00	100.00
Very High	17	16	15	94.12	93.75
Total =	50	50	40		
Overall classification Accuracy = 94.58%					
Overall Kappa Statistics = 0.8919					
Accuracy Study under Saturated Condition					
Very low	0	4	0	0.00	0.00
Low	0	7	5	0.00	71.43
Moderate	12	7	6	58.33	85.71
High	16	13	11	81.25	84.62
Very High	22	16	16	72.73	100
Total =	50	50	38		
Overall classification Accuracy = 85.44%					
Overall Kappa Statistics = 0.8919					

CONCLUSION

In the present work, my approach is to determine the potential instability location in connection to spatial distribution of geotechnical parameters. There is no any unique and generalized model available for the preparation of slope instability distribution map as the instability condition depends upon various factors which vary from one place to others. So, one simple model could not be accepted for all landslide locational sites. Considering all the landslide triggering factors of the study area, one dimensional slope stability model has been adopted to conceive the spatial distribution of slope instability. Based on the analysis priority could be fixed up for different slope instability areas and management options could be followed up for the Shivkhola watershed. It is observed from the study that the areal extent of potential slope instability and the chances or probability of slip under saturated condition is very high as a result of soil saturation and increased pore water pressure, less cohesion, and low friction angle. The large part of the watershed shows high to very high landslide susceptibility under saturated condition followed by semi-saturated and dry condition. Steep slope sites i.e. Paglajhora (lower and upper), Tindharia, Nurbong, Shiviter and Mahanadi are very much subjected to slope instability. The mid-central steep slope of the watershed must be brought under immediate attention as the propensity of areal increase in slope failure is very high as a result of drainage concentration and the percolation of water through weak lithological composition. The prepared maps may offer useful tool for the installation and the continuous monitoring of the geotechnical attributes measuring apparatus/instruments such as field shear box to assess the shear

Research Article

strength properties of the soil, permeameter, double ring infiltrometer, and piezometer to measure soil pore water pressure and to execute the landslide warning system. The monitoring result must be served to the local Govt. and the local people are to be made aware of the triggering geotechnical factors and in the same time they are to be brought into the active monitoring and management system.

REFERENCES

- Anabalagan R (1992).** Landslide hazard evaluation and zonation mapping in mountainous terrain. *Engineering Geology* **32** 269-277.
- Bhattarai P and Aoyama K (2001).** Mass Movement problems along Prithwi Highway Nepal. *Annual Report of Research Institute for Hazards in Snowy Areas, Niigata University* **23** 85-92.
- Billings MP (1987).** Structural Geology Prentice Hall of India Private Limited New Delhi-110001 3rd Edition. (Nov. 1987).
- Borga et al., (1998).** Shallow Landslide hazard assessment using a physically based model and digital elevation data. *Journal of Environmental Geology* **35**(2-30) 81-88
- Brardinoni F and Church M (2004).** Representing the Landslide Magnitude Frequency Relation; Capilano river basin British Colombia. *Earth Surface processes and Landforms* **29**(1) 115 – 124.
- Brudsen D (1979).** Mass Movement in Process in geomorphology Edited By Embelton C and Thornes J John Wiley & sons 130 – 186.
- Burton A & Bathurst JC (1998).** Physically based modeling of shallow landslide erosion and sediment yield at a catchment scale. *Environmental Geology* **35**(2-3) 89-99.
- Carrara et al., (1991).** GIS technique and statistical models in evaluating landslide hazard. *Earth Surface Process and landforms* **16**(5) 427-445.
- Carson MA (1975).** Threshold and characteristic angles of straight slopes. *Proceedings of the 4th Guelph Symposium on Geomorphology Norweich Geo Books* 19-34.
- Carson M A (1977).** Angles of repose, angles of shearing resistance at angle of talus slopes, *Earth surface Processes* **2** 363 – 380.
- Cernnica JN (1995).** “Geo-technical engineering: Soil mechanics”. *John Willy & Sons Inc.*
- Congalton R (1991).** A review of assessing the accuracy of the classification of remotely sensed data. *Remote Sensing of Environment* **37** 35-46.
- Crozier M J (1986).** Landslides: Causes, Consequences and Environment. *Croom Helm Australia Pty Ltd. London United Kingdom* 252.
- Deoja et al., (1991).** Mountain risk engineering handbook. *International Centre for Integrated Mountain Development Kathmandu* 875.
- De Vleeschauwer C and De Smedt F (2002).** Modeling slope stability using GIS on a regional scale, Proceedings of the first Geological Belgica International Meeting Leuven 11-15 September 2002. *Aardkundige Mededelingen* **12** 253-256.
- De Smedt F (2005).** Slope Instability analysis using GIS on a regional scale: a case study of Narayanghat-Mungling highway section Nepal. A dissertation report presented at *Universiteit Gent Vrije Universiteit Brussel Belgium*.
- Dhakal et al., (2000).** Landslide hazard mapping and its evaluation using GIS: An investigation of sampling schemes for a grid-cell based quantitative method. *Photogrametric Engineering & Remote Sensing* **66**(8) 981-989.
- Gao J (1993).** Identification of topographic settings conducive to landsliding from DEM in Nelson County VA USA. *Earth surface process and landforms* **18** 579-591.
- Glade T (1998).** Establishing the frequency and magnitude of landslide-triggering rainstorm events in New Zealand. *Environmental Geology* **35** 160-174.
- Guzzetti F, Cardinali M, Reichenbach P and Carrara A (1999).** Comparing landslide maps a case study in the upper Tiber River Basin central Italy. *Environmental Management* **18** 623-633.

Research Article

- Guzzeti F, Cardinali M, Reichenbach P and Carrara A (1999b).** Landslide hazard evaluation: an aid to a sustainable development *Geomorphology* **31** 181-216.
- Guzzeti F, Cardinali M, Reichenbach P, Ardizzone F and Galli M (2003).** Impact of landslides in the Umbria region central Italy. *Natural Hazards and Earth System Science* **5** 1-17.
- Hammond et al., (1992).** “Level I stability analysis (LISA) Documentation for Version 2”. General Technical Report INT-285 USDA forest Service. *Intermountain Research Station* 121.
- Montgomery DR and Dietrich WE (1989).** “Source areas, drainage density and channel initiation”. *Water Resources Research* **25**(8) 1907-1918
- Montgomery DR and Dietrich WE (1994).** A physically based model for the topographic control on shallow land sliding. *Water Resources Research* **30**(4) 1153-1171.
- Pack RT, Tarboton DG and Goodwin CN (1998).** Terrain stability mapping with SINMAP Technical description and users guide for version 1.00 Report and software. Available: <http://www.engineering.usu.edu/dtarb/>(last access: 15th June, 2007).
- Soeters R and Westen CJ (1996).** Slope instability recognition, analysis and zonation. In AK Turner and RL Schuster (Eds.). *Landslides: Investigation and Mitigation. Transportation Research Board Special Report* **247** 129-177.
- Terzaghi K (1950).** Mechanism of landslides, in Application of Geology to Engineering Practice. Barkley Volume *Geological Society of America* 83-123.
- Tiwari B and Marui H (2001).** “Shearing behaviour of landslide sliding and mining scarp soil during drained ring shear test”. *Proceedings of XV th International Conference on Soil Mechanics and Geotechnical Engineering Istanbul* **1** 295-298.
- Tiwari B and Marui H (2002).** Mechanism of shear zone formation and its effect in residual shear strength Proceedings of 3rd International Conference on Landslides *Slope Stability and Safety of Infrastructure* **1** 4-133.
- Tiwari B and Marui H (2003).** Estimation of residual shear strength for bentonite-kaolin-Toyouura sand mixture. *Journal of Japan Landslide Society* **40**(2) 124-133.
- Tiwari B and Marui H (2004).** Objective oriented multi-stage ring shear test for the shear strength of the landslide soil. *Journal of Geotech and Geoenvironmental Engineering ASCE* **130**(2) 217-222.
- Varnes DJ (1958).** Landslide types and processes, in Eckel, E. B., ed., *Landslides engineering practice: Highway Research Board Special Report 29 NAS-NRC Publication* **544** 20-47.
- Vanmarcke EH (1977).** “Reliability of Earth Slopes”. *Journal of the Geotechnical Engineering Division ASCE* **103** (GT11).
- Waltham T (2002).** Foundations of Engineering Geology.
- Windisch EJ (1991).** “The hydraulics problem in slope stability analysis”. *Canadian Geotechnical Journal* **28**(6) 903-909.
- Wu W and Siddle RC (1995).** A distributed slope stability model for step forested basins *Water Resour. Res.*, **31** 2097-2110.
- Young A (1963).** Deductive models of slope evolution Rep. Int. Geogr. Un. Slopes. *Commission* **3** 45-66.
- Zaruba Q and Mencl V (1982).** *Landslides and Control* Elsevier Scientific Publishing Company 52 Vanderbilt Avenue New York 10017 **324** 35.